JOURNAL OF MATERIALS SCIENCE 31 (1996) 6299–6304

Study of growth dislocations in L-arginine phosphate monohydrate single crystals by chemical etching

K. SANGWAL
Department of Physics, Technical University of Lublin, ul. Nadbystrzycka 38, 20-618 Lublin, Poland

S. VEINTEMILLAS-VERDAGUER
Institut de Ciencia dels Materials de Barcelona, CSIC, Campus de la UAB, 08193 Bellaterra, Spain

J. TORRENT-BURGUÉS
Department d'Enginyeria Quimica, Universitat Politecnica de Catalunya, Colom 1, 08222 Terrassa, Spain

The results of a study of the distribution of growth dislocations revealed on different faces of L-arginine phosphate monohydrate (LAP) crystals by selective etching in relation to the growth conditions of the crystals are described. It was found that (1) the dislocation density, ϱ, on a face is the highest in its central regions and depends on the supersaturation used for growth, and that (2) ϱ on different faces is different. The observations are discussed from the standpoint of the mechanism of generation of dislocations at the seed–crystal interface in the initial stages of regeneration of the seed and at the crystal–medium interface due to the formation of bunches of growth layers on the growing crystal faces during their development.

1. Introduction

Non-linear optical L-arginine phosphate monohydrate (LAP) crystallizes in the monoclinic system with space group $P2_1$ with two formula units per cell and has cell dimensions $a = 1.085$ nm, $b = 0.791$ nm, $c = 0.732$ nm and $\beta = 98.0°$ [1]. Its growth was first reported by Eimerl *et al.* [2] and Yokotani *et al.* [3], but a systematic study of its growth, growth habit and characterization of dislocations by Lang topography was carried out by Dhanaraj *et al.* [4]. These authors [4] grew LAP crystals by solvent-evaporation and temperature-lowering methods and found that the crystals grown by the solvent-evaporation method contained a very high dislocation density in comparison with those grown by the temperature-lowering method.

The main limitations of the Lang topography in studying the distribution of dislocations, are poor resolution and preparation of not-too-thick slices of appropriate orientations [5, 6]. Owing to the poor resolution achieved, only crystals containing a relatively low dislocation density (less than 10^4 lines cm^{-2}) may be studied, while the requirement of sample preparation does not allow one to obtain quantitative information about the global distribution of dislocations on an as-grown face along different directions and to compare the density of dislocations emerging on different faces present in the growth morphology. Therefore, in contrast to X-ray topography, selective etching is more appropriate for the study of distribution and density of dislocations in crystals because it does not require sample preparation, and crystals having dislocation densities up to 10^7 lines cm^{-2} can routinely be studied using a standard optical microscope.

The experimental results of a study of the distribution of growth dislocations revealed on different faces of LAP crystals by selective etching in relation to the growth conditions of the crystals, are described and discussed in this paper.

2. Experimental procedure

The LAP crystals for etching studies were grown from aqueous solutions by the solvent-evaporation method on self-nucleated seeds and by the constant-temperature constant-supersaturation method on seeds. In the growth experiments by the former method, 600 g 20% LAP solution was placed in a 1 l crystallization dish kept in a thermostated desiccator, and growth was carried out at about 40 °C by solvent evaporation ensured by a small nitrogen stream flowing over the solution. After a period of about 1 week, the crystals were taken out of the solution and dried between filter papers. In the latter method, the experimental apparatus for growth was similar to that described by

Dhanaraj *et al.* [4]. The crystals were grown on small seeds at a constant temperature of 38 °C from solutions of desired supersaturations contained in coloured growth vessels. The desired supersaturation used for growth was calculated from the reported solubility data [4]. For crystal growth by this method, the seeds were initially prepared by the solvent-evaporation method, and the selected ones were mounted in specially designed holders [7]. Bending by about 30° in the rod containing the seed holder, and rotation of the whole assembly by an electric motor, provided stirring of the solution relative to the growing crystal. A thick *n*-hexane layer was placed above the supersaturated solutions. After a desired period of growth, the crystal was withdrawn from the supersaturated solution through the *n*-hexane layer and dried between filter papers.

In order to investigate the distribution and density of dislocations emerging on different faces, the as-grown faces of LAP crystals grown by the above two methods were etched at room temperature (23 °C) for known durations in distilled water, methanol and ethanol. These three solvents produce etch pits at the sites of dislocations emerging on different faces of LAP crystals [8]. After etching, the etched surfaces were dried between filter papers and examined under a Nikon optical microscope.

The densities of dislocations emerging on different faces and in different regions of a given face were calculated from etch pit counts in 30 cm^2 areas on photographs made at high magnifications (4.5 times the magnification of the original negatives). Regions containing clusters or an enormously high density of dislocation etch pits in the vicinity of macrospirals emerging on a face, were excluded in the etch-pit counts. Corresponding to a particular distance, l, from a reference edge of the face of width, L, in a particular direction the relative distance X was calculated as l/L.

3. Distribution of dislocations on as-grown $\{100\}$, $\{110\}$ and $\{101\}$ faces

The LAP crystals obtained by solvent evaporation were somewhat yellowish in colour and usually contained microbes, while those obtained by solvent evaporation at 40–50 °C in a nitrogen stream and by the constant-temperature constant-supersaturation method were colourless and free from microbes. These characteristics of the crystals obtained by the two methods are in agreement with the observations made by earlier workers [3, 4].

The LAP crystals grown by us showed growth morphologies very similar to those reported by Dhanaraj *et al.* [4]. The $\{100\}$, $\{110\}$, $\{101\}$, $\{011\}$ and $\{111\}$ faces were observed to be the morphologically important faces on the crystals. The typical habit of an LAP crystal grown from aqueous solutions is shown in Fig. 1.

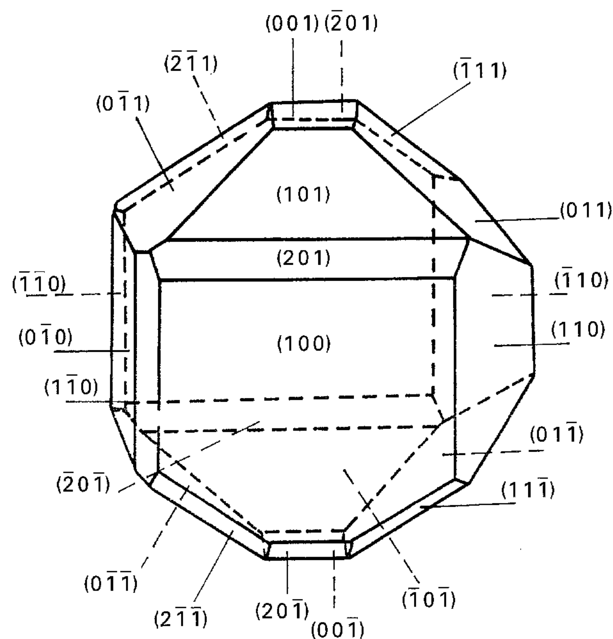

Figure 1 Typical habit of an LAP crystal grown from aqueous solutions.

Fig. 2a and b illustrate the distribution of dislocation etch pits observed along the $\langle 001 \rangle$ directions on the $(\bar{1}00)$ and (100) face of LAP crystals grown at 6% and 10% supersaturations, respectively. The regions of the photographs are close to the edges of the above faces with the neighbouring $(\bar{1}00)$ and $(0\bar{1}0)$ faces, respectively (see Fig. 1). One may note from Fig. 2a and b that the dislocation density is the lowest in regions close to the $(\bar{2}01)$ and $(20\bar{1})$ faces, respectively, which always appear in the morphology, i.e. whose morphological importance is relatively insensitive to the supersaturation used for growth, and that it increases progressively in the direction of $(\bar{2}0\bar{1})$ and (201) faces which develop at high supersaturations. However, the pit density somewhat decreases after some distance from the region of the highest dislocation density.

The distribution of dislocation etch pits observed along $[010]$ and $[00\bar{1}]$ directions on the $(\bar{1}00)$ and $(\bar{1}10)$ faces of an LAP crystal grown at 10% supersaturation is shown in Fig. 3a and b, respectively. Fig. 3a shows that the pit density is the highest in regions close to the seed holder and steadily decreases in the $[0\bar{1}0]$ direction as one goes away from the seed holder, while in Fig. 3b the pit density along the $[001]$ direction first increases and then decreases.

The above results of the highest dislocation density in the central regions of a face (Figs 2a, b and 3b) and in regions close to the regenerated seed (Fig. 3a), are qualitatively in agreement with the observations made by X-ray topography [9–11]. However, in order to obtain precise information about the distribution of dislocations emerging on different faces, quantitative data on dislocation density from etch-pit counts in different regions of the faces were obtained. The results of the dependence of dislocation etch-pit density, ϱ, against relative distance, X, for different faces of LAP crystals grown at 10% and 6% supersaturations, are presented in Fig. 4a and b, respectively. The data on pit densities calculated from the photographs in Figs 2 and 3 are also included in this figure. In the

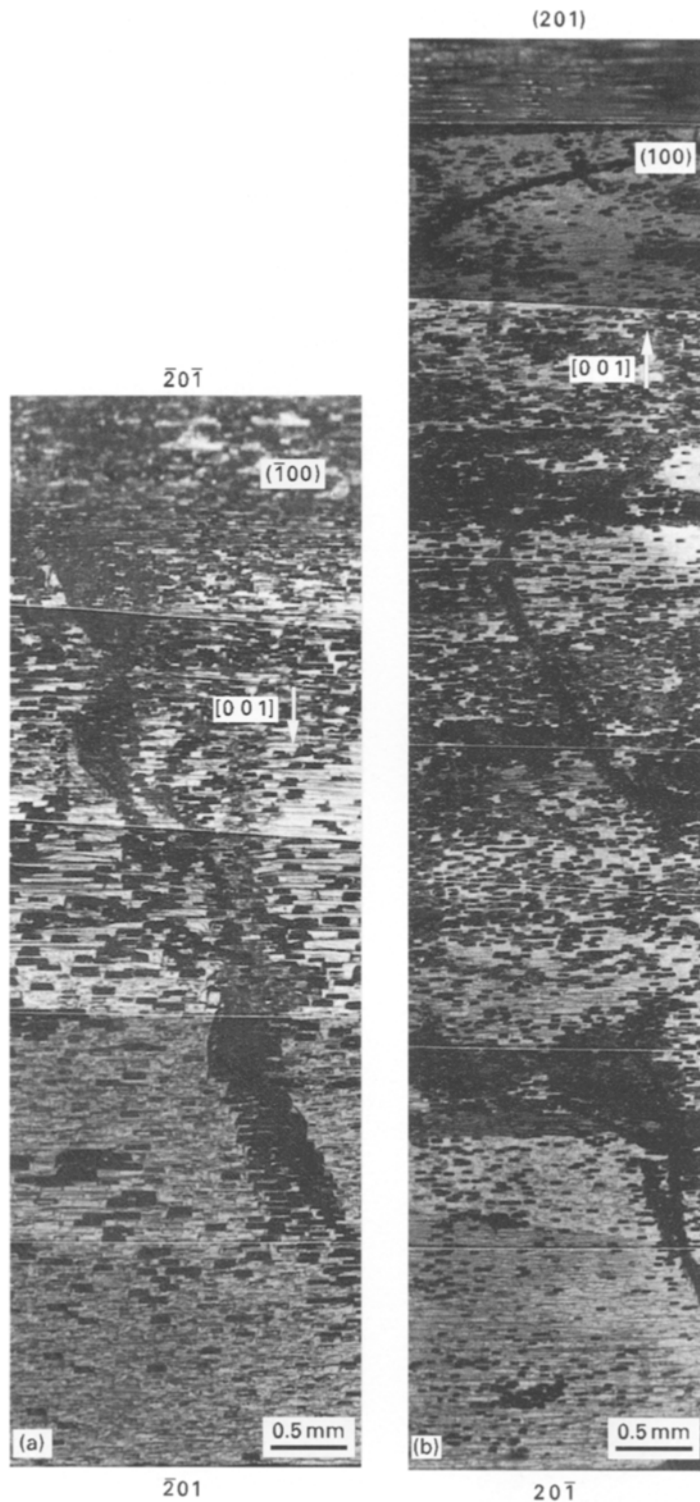

Figure 2 Distribution of dislocation etch pits observed along the ⟨001⟩ direction on the (a) ($\bar{1}$00) and (b) (100) face of LAP crystals grown at 6% and 10% supersaturations. The regions of the photographs are close to the edges of the above faces with the neighbouring ($\bar{1}$10) and (0$\bar{1}$0) faces, respectively. Edges of the faces with ($\bar{2}$01) and (201) faces are shown in the figures.

plots of Fig. 4, the origin $X = 0$ corresponds to the edge of the region of the lowest etch-pit density on a face.

As seen from Fig. 4, the dependence of ϱ on X for different faces of LAP, in general, reveals three regions:

1. for $X < X_0$, ϱ is independent of X (Figs 2 and 3);
2. for $X_0 < X < X_{max}$, ϱ increases with X (Figs 2 and 3);
3. for $X > X_{max}$, ϱ decreases with an increase in X (Figs 2a, b and 3b).

In order to describe the dependences of ϱ on X, linear, exponential and logarithmic functions were tried. It was found that in both regions 2 and 3, the following linear functions give the best fit:

for $\varrho < \varrho_{max}$

$$\varrho = \varrho_0 + A(X - X_0) \quad (1)$$

and for $\varrho > \varrho_{max}$

$$\varrho = B(1 - X) - \varrho_0. \quad (2)$$

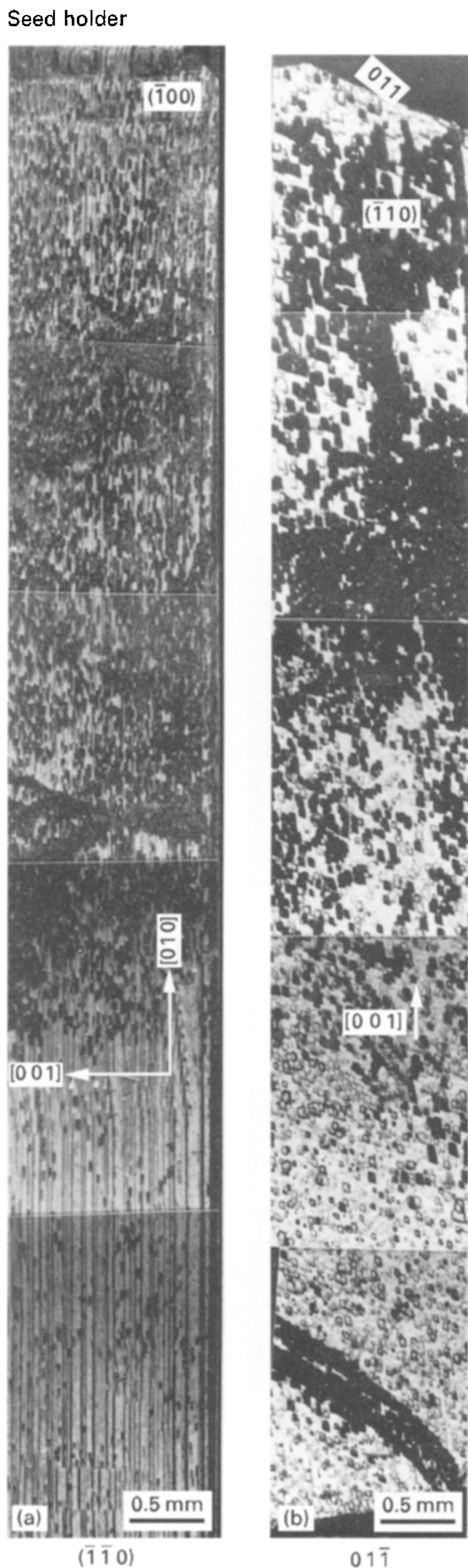

Figure 3 Distribution of dislocation etch pits observed along [0 1 0] and [0 0 1] directions on (a) (1̄ 0 0) and (b) (1̄ 1 0) faces of an LAP crystal grown at 10% supersaturation. In (a) the position of the seed holder is situated close to the top of the figure.

where ϱ_0 is the constant value of the density of dislocations on a face in the ascending part of the curve (i.e. for $X < X_0$), ϱ_0' is the dislocation density for $X = 1$ in the descending part of the curve, and A and B are the slopes of the ascending and the descending parts of the $\varrho(X)$ curves. The values of these parameters are listed in Table I.

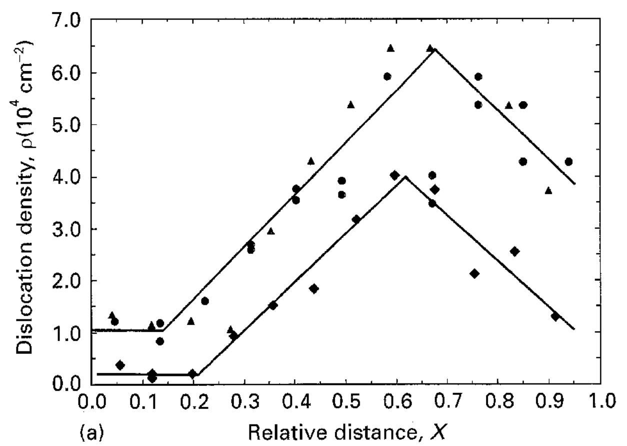

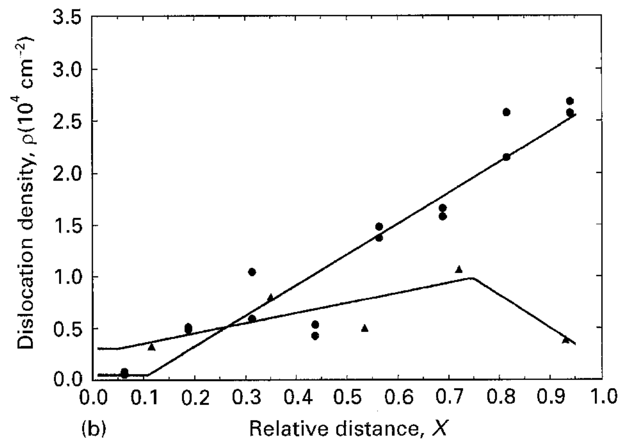

Figure 4 Plots of dislocation etch-pit density, ϱ, against relative distance, X, for different faces of LAP crystals grown at (a) 10% and (b) 6% supersaturations. (a) (●) (1 0 0), (▲) (1̄ 0 0) and (◆) (1̄ 1 0) faces; (b) (●) (1̄ 0 0) and (▲) (1 0 1) faces. The data on pit densities calculated from the photographs of Figs 2 and 3 are shown in this figure.

Examination of the plots of the dislocation density, ϱ, against X, illustrated in Fig. 4, reveals that, apart from its dependence on X, the dislocation density at a particular X depends on the supersaturation, σ, used for growth and on the type of the face. A better insight into the processes responsible for these dependences may be obtained by considering the values of different parameters listed in Table I.

Table I reveals that the values of the dislocation densities ϱ_0 and ϱ_0', and the slopes A and B increase with supersaturation, and, at a given supersaturation, depend on the growth face. Moreover, $\varrho_0' \geqslant \varrho_0$. The values of these parameters are essentially associated with the mechanism of generation of dislocations perpendicular to the seed–crystal interface during the regeneration stage of the seed and with the process of formation of bunches on a face during its development.

As observed in several works (for example, see [12] for the literature), bunching of elementary layers emitted from a source progressively increases as one goes away from the layer source. Denoting the thickness of bunching layers by h, the relationship between h and X may be given by

$$h \propto X^{1/2}, \quad (3)$$

TABLE I Estimated values of different parameters of Equations 1 and 2

σ(%)	Face	$X < X_{max}$			$X > X_{max}$		$\varrho_{max}(cm^{-2})$
		$\varrho_0(cm^{-2})$	X_0	$A(cm^{-2})$	$\varrho'_0(cm^{-2})$	$B(cm^{-2})$	
6	$(\bar{1}00)$	5.0×10^2	0.11	3.0×10^4	–	–	2.7×10^4
	(101)	3.0×10^3	0.05	1.0×10^4	2.0×10^3	3.2×10^4	9.7×10^3
10	$(100), (\bar{1}00)$	1.1×10^4	0.14	1.0×10^5	3.0×10^4	9.3×10^4	6.3×10^4
	$(\bar{1}10)$	2.0×10^3	0.21	9.4×10^4	6.6×10^3	8.7×10^4	4.3×10^4

and

$$h \propto \ln(X/X_0) \quad (4)$$

according to Chernov's [13] and Van der Eerden and Müller-Krumbhaar's models [14], respectively. In Equation 4, X_0 now denotes the distance when bunching sets in on a face. Because it may be assumed that an increase in the dislocation density due to bunching is proportional to h, one may conclude that none of the above equations describes the dependence of ϱ on X satisfactorily in the ascending and descending parts of the $\varrho(X)$ curves. However, of the two relations, Equation 4 is probably closer to the linear dependence for the approximation $\ln x = x - 1$. Then ϱ_0 and ϱ'_0 are the densities of dislocations generated normal to the growing face by the bunching process.

It is well known [9, 11] that during the regeneration stage of a seed, dislocations are generated perpendicular to the seed–crystal interface and the density of these dislocations increases with supersaturation. Therefore, we may assume that the dislocations thus generated at the seed–crystal interface, emerge on a face and participate in its growth. If ϱ_{max} is the density of these dislocations emerging on a face, the slopes $A = (\varrho_{max} - \varrho_0)/(X_{max} - X_0)$ and $B = (\varrho_{max} - \varrho'_0)/(1 - X_{max})$ determine the gradients of the generation of dislocations emerging on the growing face of a crystal in the ascending and descending parts of the $\varrho(X)$ plots, and are associated with the bunching of growth layers originating from the dislocation source. Moreover, if the displacement rates of layers on a face, and consequently the formation of bunches and generation of dislocations therefrom, are different in opposite directions, the slopes A and B are expected to be different and depend on the supersaturation used for growth and on the type of growing face. For example, on the (1 0 0) face, the layer displacement rate is several times greater in the $[00\bar{1}]$ direction than that in the [0 0 1] direction, and bunch formation is more intense in the latter direction [15]. Thus, the differences in the dislocation densities ϱ_0 and ϱ'_0, and in the slopes A and B increase with increasing supersaturations when bunching becomes increasingly pronounced. Therefore, it may be concluded that the values of ϱ_{max}, ϱ_0 and ϱ'_0 depend on the supersaturation used for growth and on the type of growing face. The calculated values of ϱ_{max} for the (1 0 0), (1 0 1) and $(\bar{1}10)$ faces are included in Table I.

The above ideas of the generation of dislocations in terms of bunch formation on a face during their growth can also be extended to explain the dependence of ϱ on X for the (1 0 0) face of Fig. 4b, in which the source of layers is in the vicinity of the seed holder. In these cases, one observes groups of tiny etch pits composing large pits formed at bundles of dislocations. An example of such etch pits observed on the $(\bar{1}00)$ face of an LAP crystal grown at 6% supersaturation, is shown in Fig. 5.

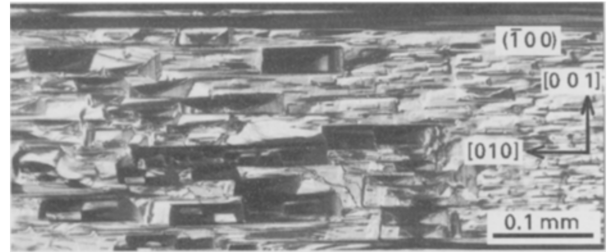

Figure 5 Example of etch pits composed of tiny etch pits on the $(\bar{1}00)$ face of a crystal grown at 6% supersaturation.

4. Dislocation densities on different as-grown faces

As mentioned above (see Fig. 4), the dislocation density depends on the supersaturation used for growth as well as on the type of the face. Fig. 6a and b show examples of etch-pit patterns produced on the $\{\bar{2}01\}$ faces of LAP crystals grown at 6% and 10% supersaturations, while Table II gives the dislocation etch-pit densities in randomly selected areas of various faces of LAP crystals grown under different conditions.

Examination of Figs 4 and 6, and Table II reveals that the density of dislocations, ϱ, strongly depends on the face as well as on the growth conditions. For example, in the case of crystals grown by the constant-temperature constant-supersaturation method, the density of dislocations emerging on a particular face of the crystals grown at 6% supersaturation is roughly an order of magnitude lower than that in the case of the crystals obtained at 10% supersaturation. Similarly, the dislocation density in crystals grown by solvent evaporation is even greater than that in crystals grown at 10% supersaturation.

The process of generation of dislocations depends on the value of supersaturation used and on the energy of formation of a dislocation normal to a face in the direction of its displacement. Because the Burgers

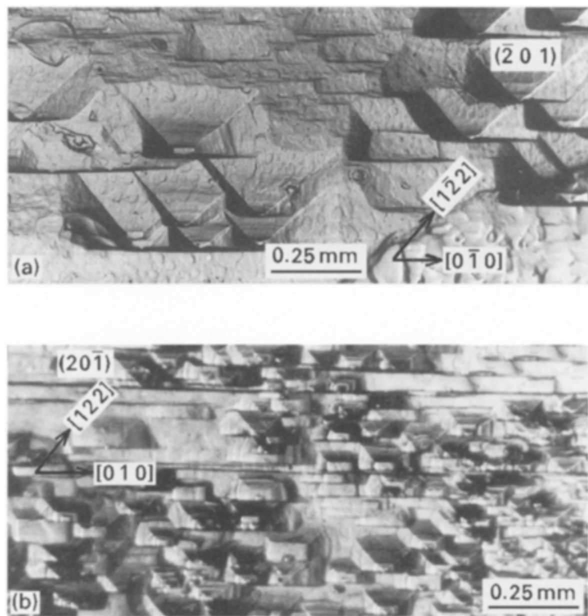

Figure 6 Etch-pit patterns produced on the $\{\bar{2}01\}$ face of LAP crystals grown at (a) 6% and (b) 10% supersaturations. A much higher pit density in (b) is clearly seen.

TABLE II Dislocation etch-pit densities on different faces of LAP crystals grown under different conditions

Face	d_{hkl}	Constant supersaturation		Solvent evaporation at 40 °C
	(10^{-10} m)	6%	10%	
{1 0 0}	10.74	5×10^3	$4–5 \times 10^4$	$5–8 \times 10^4$
{1 1 0}	6.37	$1–2 \times 10^4$	1×10^5	$6–10 \times 10^5$
$\{1\bar{1}0\}$		$4–9 \times 10^3$	$2–5 \times 10^4$	–
{1 0 1}	5.66	$3–8 \times 10^3$	$4–7 \times 10^4$	4×10^4
{0 0 1}	7.25	4×10^3	2×10^4	$1–10 \times 10^4$
{0 1 1}	5.34	–	$3–6 \times 10^3$	–
$\{01\bar{1}\}$		$3–8 \times 10^3$	9×10^4	$4–10 \times 10^4$
$\{\bar{2}01\}$		2×10^3	–	–
{2 0 1}	4.64	2×10^4	5×10^3	–
{1 1 1}	4.99	1×10^3	2×10^4	–

vector, $\boldsymbol{b}$, of a dislocation line is usually equal to the interplanar distance, d_{hkl}, and the dislocation energy is proportional to $\boldsymbol{b}^2$, an inverse relation between ϱ_0 and d_{hkl} may be expected. As suggested by Table II, there is no relation between dislocation density and interplanar distance. Therefore, the dependence of the observed dislocation density, ϱ, on growth conditions in Table II may be attributed to the combined effect of the process of generation of dislocations at the crystal–medium interface during the initial stages of growth as well as on the bunching of layers emitted by the dislocation source during the development of a face.

5. Conclusions

1. The distribution of dislocations observed on different mophologically most important faces of LAP crystal grown by the constant-temperature constant-supersaturation method is non-uniform, the maximum dislocation density being in the central regions of the faces.

2. The density of dislocations on different faces of LAP crystals is different and depends both on the method of growth and on the supersaturation used for growth. The dislocation density in the crystals grown by the constant-temperature constant-supersaturation method is lower than in the crystals grown by the solvent-evaporation method at 40 °C. Even in the case of the former method, the crystals grown at low supersaturations have relatively low dislocation density.

Acknowledgement

This work was partly financed by CICYT Project MAT92-0263-C02-01.

References

1. K. AOKI, K. NAGAMO and Y. IITAKA, *Acta Crystallogr.* **B 27** (1971) 11.
2. D. EIMERL, S. VELSKO, L. DAVIS, F. WANG, G. LOIACONO and G. KENNEDY, *IEEE J. Quant. Electron.* **25** (1989) 179.
3. A. YOKOTANI, T. SASAKI, K. FUJIOKA, S. NAKAI and T. YAMANAKA, *J. Crystal Growth* **99** (1990) 815.
4. G. DHANARAJ, T. SHRIPATHI and H. L. BHAT, *ibid.* **113** (1991) 456.
5. S. AMELINCKX, "Direct Observations of Dislocations", Supplement to *Solid State Phy.* **6** (Academic Press, New York, 1964).
6. K. SANGWAL, "Etching of Crystals: Theory, Experiment and Application" (North-Holland, Amsterdam, 1987).
7. K. SANGWAL, R. RODRIGUEZ-CLEMENTE and S. VEINTEMILLAS-VERDAGUER, *J. Crystal Growth* **78** (1986) 144.
8. K. SANGWAL, S. VEINTEMILLAS-VERDAGUER and J. TORRENT-BURGUES, *ibid.*, **154** (1995) 364.
9. M. C. ROBERT and F. LEFAUCHEUX, *ibid.*, **65** (1983) 637.
10. H. KLAPPER, in "Characterization of Crystal Growth Defects by X-ray Methods", edited by B. K. Tanner and D. K. Bowen (Plenum, New York, 1978) p. 133.
11. J. N. SHERWOOD and T. SHRIPATHI, *J. Crystal Growth* **88** (1988) 358.
12. K. SANGWAL and R. RODRIGUEZ-CLEMENTE, "Surface Morphology of Crystalline Solids" (Trans Tech, Zurich, 1991) Ch. 3.
13. A. A. CHERNOV, *Sov. Phys. Uspekhi* **4** (1961) 116.
14. J. P. VAN DER EERDEN and H. MÜLLER-KRUMBHAAR, *Electrochim. Acta* **31** (1986) 1007.
15. K. SANGWAL, S. VEINTEMILLAS-VERDAGUER and J. TORRENT-BURGUES, *J. Crystal Growth* **155** (1995) 135.

Received 10 April 1995
and accepted 13 June 1996